Electronic Supplementary Material (ESI) for Physical Chemistry Chemical Physics.

SUPPORTING INFORMATION

Charged Nanoporous Graphene Membranes for Water Desalination

Chinh Thanh Nguyen(1) and Ali Beskok(1)
1) Department of Mechanical Engineering, Southern Methodist University, Dallas, Texas 75205, USA

A. Salt distribution in stage (a) for positively charged graphene membrane

Figure S1 shows the distributions of sodium (Na^+) and chloride (Cl^-) ions in the streamwise z-direction for the charged membranes with different total applied charges in stage (a). For each case of total applied charge, the nanopore was initially blocked to fix the thermodynamic state of water at 0.997 g/cm^3 and 300 K. The concentrations of Na^+ and Cl^- ions were preserved at approximately 0.6 M in the bulk region sufficiently away from the graphene membrane regardless of the total charge fixed on the pore edge. However, Cl^- ions accumulate near the membrane whereas Na^+ ions are excluded. Due to Coulombic forces, counter-ions (Cl^-) are attracted to the positively charged nanopores, while co-ions (Na^+) are repelled. This establishes a peak of Cl^- ions near the membrane, forming an electric double layer (EDL) to balance the charges on the nanopore.

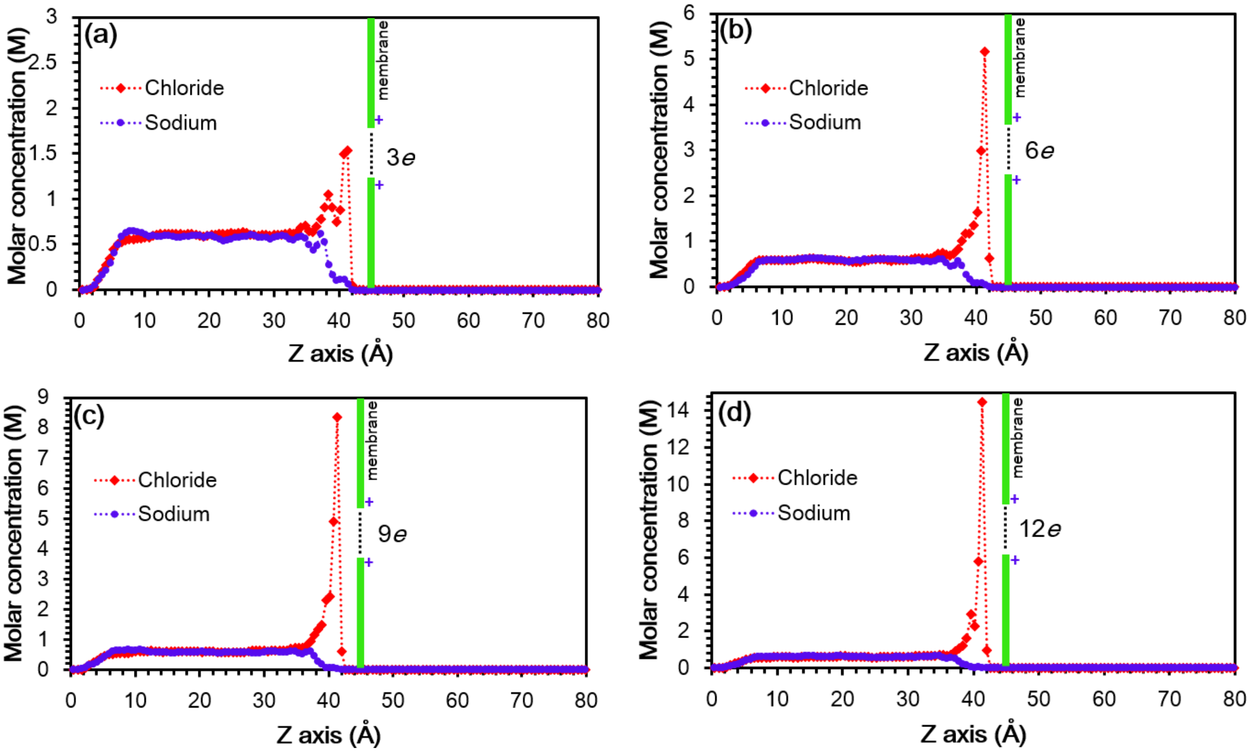

Figure S1: Distributions of sodium and chloride ions in the z-direction for positively charged graphene membranes with 3*e* (a), 6*e* (b), 9*e* (c), and 12*e* (d) total applied charge. At the first equilibrium state (stage *a*), the nano-pore is blocked, and the thermodynamic state of water is fixed at 0.997 g/cm^3 and 300 K in the feed and permeate reservoirs. Due to the use of slab-bins in z-direction, the presented ionic distributions are averaged across the entire membrane and pore areas.

B. Time evolution of water molecules in feed reservoir and flow rate results

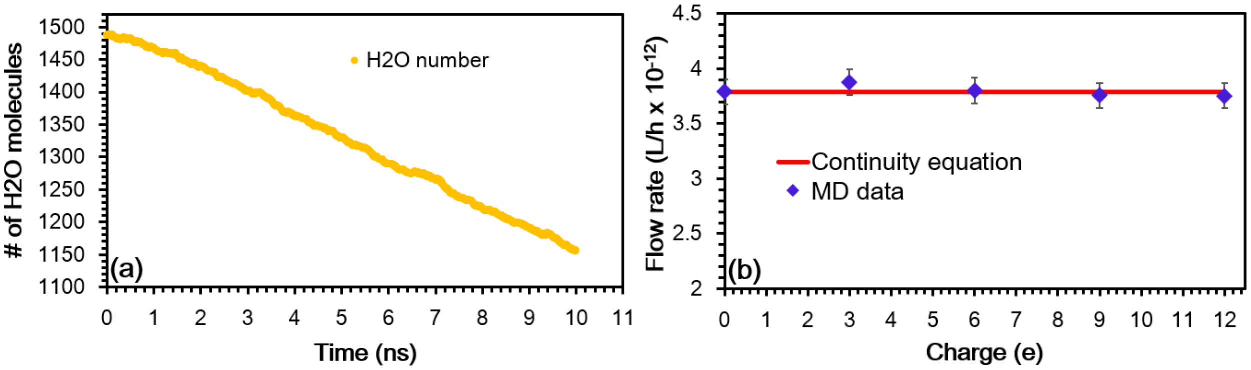

Figure S2: Time variation of the number of water molecules in the feed reservoir for the $q = 6e$ case (a). Comparisons between the volumetric flow rates obtained from MD simulations and continuity equation for different total applied charges (b). Data for $q=0e$ represents pristine graphene membrane[s1]. Flow rate was obtained using the slope of time variation of water molecules in the feed reservoir, and the standard deviation was calculated using flow rate data from *ten* different simulations with statistically different initial conditions.

In stage (c), pressure-driven flows were created through the charged nanopores by motions of the specular reflecting boundaries. The manifestation of the flow is illustrated by the time evolution of the number of water molecules in the feed reservoir as shown in **Fig. S2(a)**. The data were taken from the $q = 6e$ case for illustration purposes. Approximately 2 ns after the flow is generated, the number of water molecules in the feed reservoir decreases linearly with time. The time rate of change of water molecules number in the feed reservoir is calculated based on the slope of the data after 2 ns. The volumetric flow rate is estimated using the following equation:

$$\Phi = n \times v_{\mathrm{H_2O}} \ , \tag{S1}$$

where Φ is flow rate, n is the average rate of water molecules passing through the nanoporous membrane per unit time, and $v_{\mathrm{H_2O}}$ is the volume occupied by a water molecule (2.99×10^{-23} cm^3). **Figure S2(b)** shows the volumetric flow rate of water for different nanopore charges. The MD data for the case of pristine nanoporous graphene membrane ($q = 0e$) with the same pore diameter was obtained from Nguyen and Beskok 2018[s1]. The volumetric flow rate of water is largely unchanged with the total applied charge, and good agreement between the MD data and the flow rate obtained from the continuity equation ($Q = A \times u$, where u is the constant boundary velocity and A is the cross-sectional area of the moving boundary) is observed.

C. Radial distribution function of chloride ions near sodium ions in the reservoirs

In order to calculate the radial distribution function (RDF) in MD simulations, the neighbors around each atom or molecule are sorted into spherical distance bins. The number of neighbors in each bin is averaged over the entire simulation. **Figure S3** shows the RDF of Cl^- ions near Na^+ ions in the bulk regions of the feed and permeate reservoirs for the $q = 3e$ and $q = 9e$ cases. In the feed side, the probability of finding Cl^- ions around a Na^+ ion is high at a radial distance shorter than 3 Å, which indicates pairing between Na+ and Cl^- ions. In the permeate side, $q = 3e$ shows similar ion pairing, while the results for $q = 9e$ case show zero due to lack of Na^+ ions in the permeate reservoir. Similar behavior was observed for $q = 12e$ case, and the data is not shown for brevity.

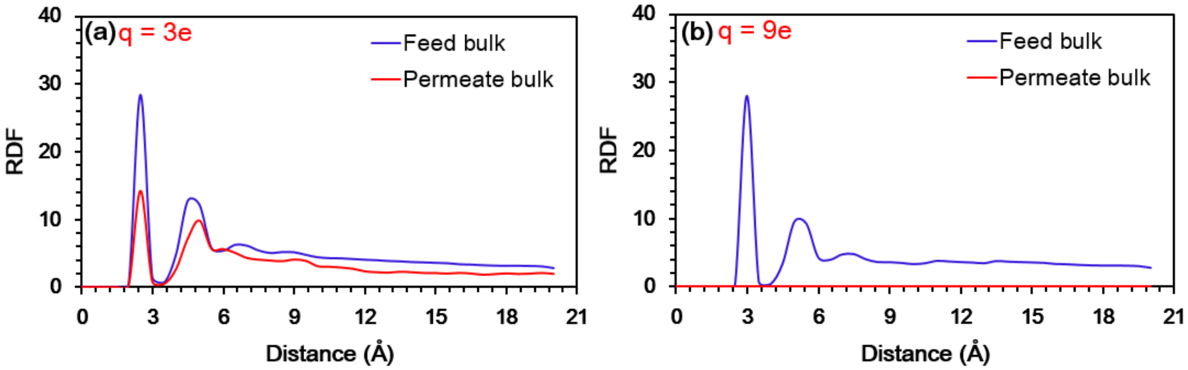

Figure S3: Radial distribution function of Cl^- near Na^+ ions in the bulk feed and permeate reservoirs for $q = 3e$ case (a) and $q = 9e$ case (b).

D. Salt distribution in stage (a) for negatively charged graphene membrane

Similar to the positively charged cases, all four negatively charged nanoporous graphene membranes (q = -3e, -6e, -9e, and -12e) were first blocked to fix the thermodynamic state of water at 0.997 g/cm^3 and 300 K. **Figure S4** shows Na^+ and Cl^- ion distributions along the z-direction at this state. The Na^+ and Cl^- concentrations in the feed reservoir were preserved at approximately 0.6 M in the bulk regions regardless of the total applied charge. Similar to the positively charged cases, we observed accumulation of counter-ions (Na^+) near the negatively charged membrane, whereas the co-ions (Cl^-) are repelled, forming an EDL on the feed reservoir side of the membrane.

We also observed the increase of counter-ion (Na^+) density peak with the increased total applied charge. Interestingly, starting from the q = -9*e* case, co-ions (Cl^-) accumulate near the peak of the counter-ions as shown in the insets of **Fig. S4(c)** and **Fig. S4(d).** This is due to excessive adsorption of counter-ions at Stern layer, leading to a larger co-ion charge density than the counter-ion charge density in the diffuse layer[s2]. This phenomenon is known as charge inversion, and it was previously reported for negatively charged surfaces with large surface charge densities[s3-s5].

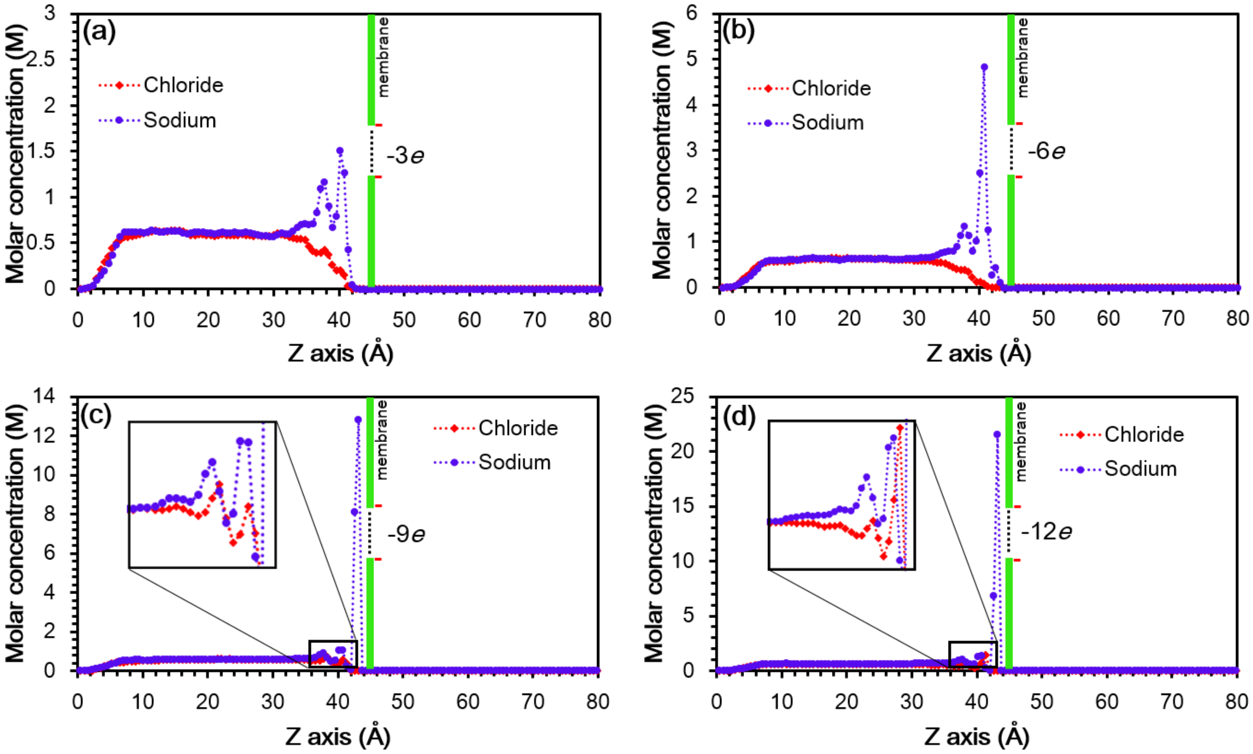

Figure S4: Distributions of sodium and chloride ions in the z-direction for negatively charged graphene membranes with -3*e* (a), -6*e* (b), -9*e* (c), and -12*e* (d) total applied charge. At the first equilibrium state (stage *a*), the nano-pore is blocked, and the thermodynamic state of water is fixed at 0.997 g/cm^3 and 300 K in the feed and permeate reservoirs. Due to the use of slab-bins in z-direction, the presented ionic distributions are averaged across the entire membrane and pore areas.

E. Salt distribution for negatively charged graphene membrane with smaller pore sizes

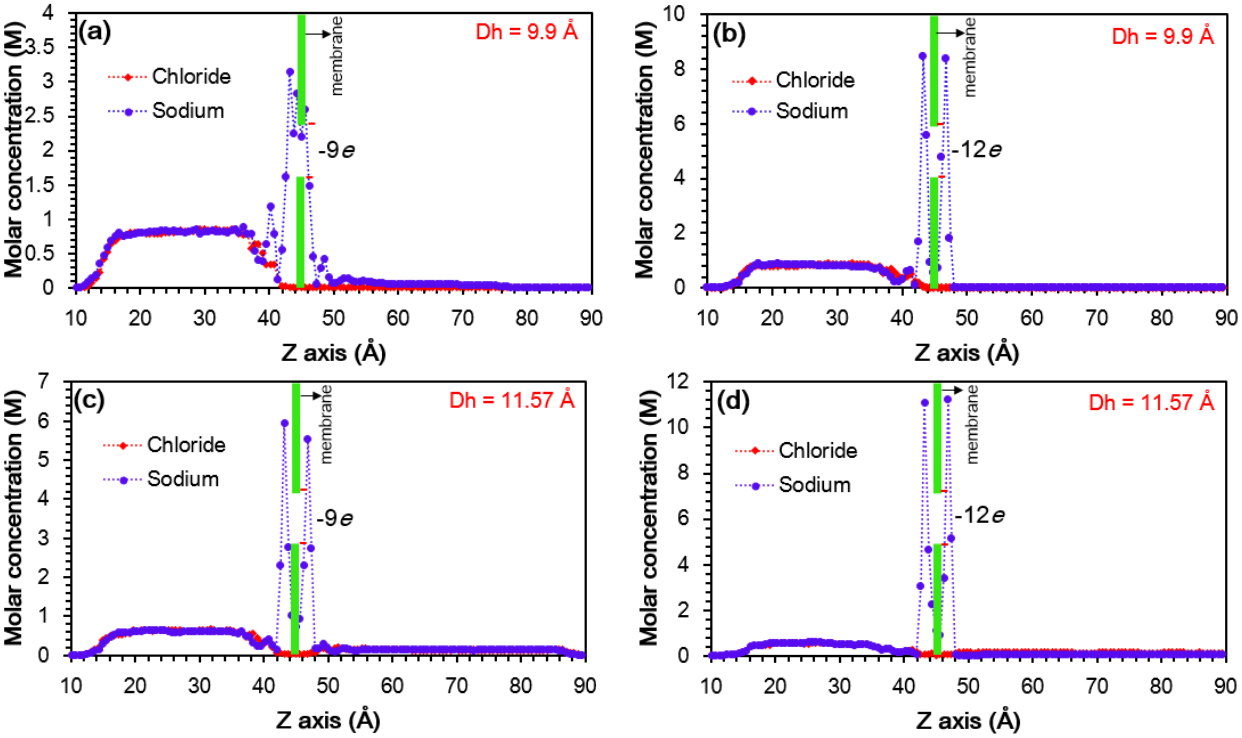

Figure S5: Distributions of sodium and chloride ions in the z-direction for negatively charged graphene membranes with q = -9e and D_h = 9.9 Å (a), q = -12e and D_h = 9.9 Å (b), q = -9e and D_h = 11.57 Å -9e (c), and q = -12e and D_h = 9.9 Å (d) at the end of flow simulations (t=10 ns in stage c). Due to the use of slab-bins in z-direction, the presented ionic distributions are averaged across the entire membrane and pore areas.

Figure S5 shows salt ion distributions in the z-direction at the end of the entire simulation time of pressure-driven flow using q = -9e and q = -12e for pore diameters of 9.9 Å and 11.57 Å. For the pore diameter of 9.9 Å, no co-ions (Cl^-) pass through the membranes, leaving the permeate reservoirs with zero Cl^- concentration for both charges. However, some counter-ions (Na^+) pass through the membranes but mostly reside near the membrane-water interfaces (**Figures S5 a, b**). For the pore diameter of 11.57 Å, small amounts of co-ions (Cl^-) and counter-ions (Na^+) pass through the membranes as in the case of 14.4 Å pore diameter, and these form a bulk concentration in the permeate reservoirs (**Figures S5 c, d**). However, a smaller number of salt ions transport through the membrane with the increased total fixed charge compared to the case of 14.4 Å pore diameter in **Figure 9c, d. Figure S6** presents Na^+ distributions in the plane containing the membrane for the mentioned cases. The Na^+ ions reside around the pore edge and the degree of localization increases with increased total applied charge. It is noted that there is not much difference between the crowding of Na^+ in the middle of the pore for q = -9e and q = -12e cases in the 11.57 Å pore. Thus, the role of Coulombic interactions is more dominant than the crowding effect at the middle of the pore, leading to reduced transport of salt ions with larger total fixed charge. Although the desalination efficiencies in these considered cases of charges and pore diameters are apparently better than the cases of 14.4 Å pore diameter, the required pressure drops

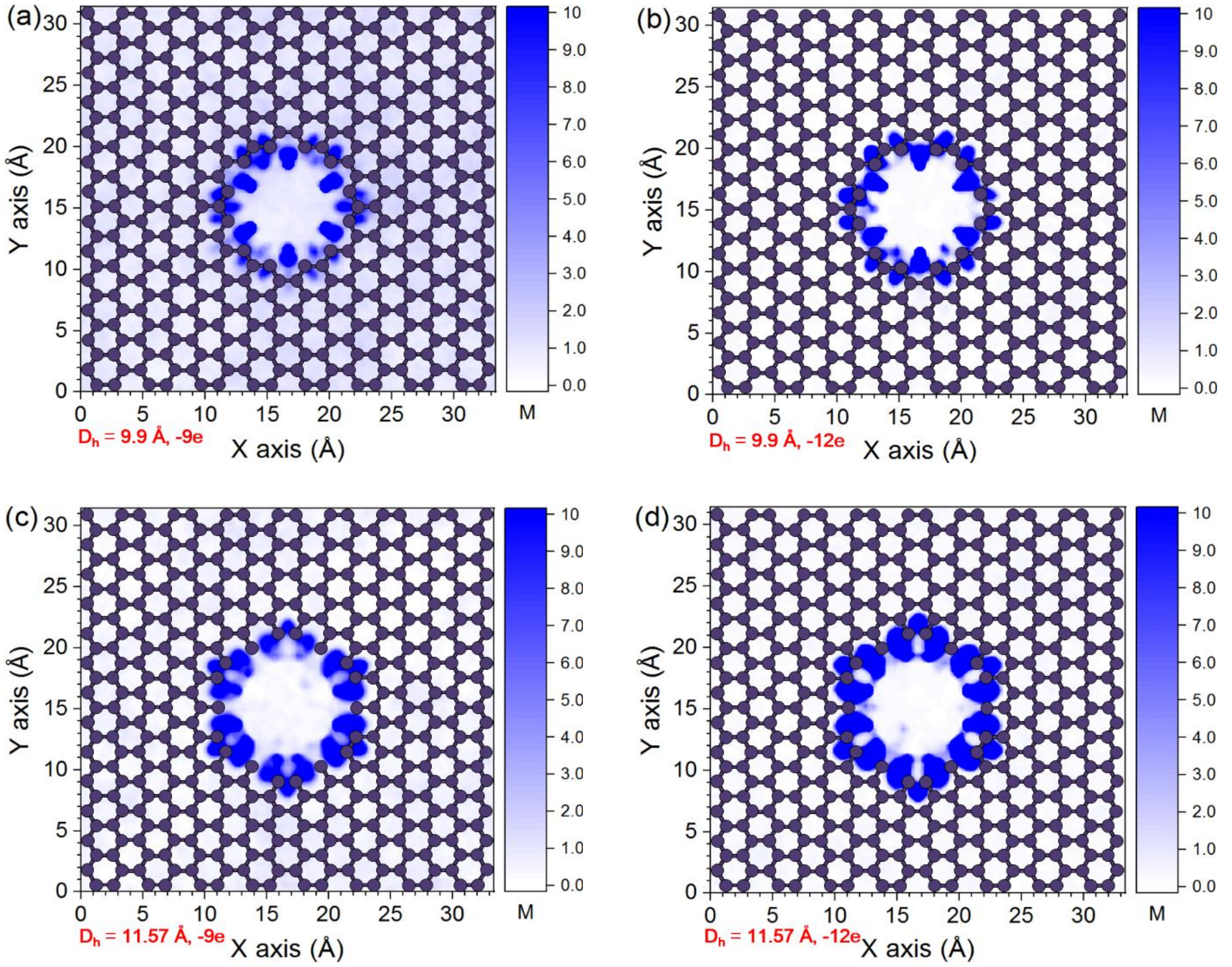

Figure S6: Distributions of sodium ions in the plane containing the negatively charged nanoporous graphene membranes with q = -9e and D_h = 9.9 Å (a), q = -12e and D_h = 9.9 Å (b), q = -9e and D_h = 11.57 Å -9e (c), and q = -12e and D_h = 9.9 Å (d) at the second equilibrium state (stage b), where the nano-pore is open but there is zero net flow. Contour colors show Na^+ concentration in M.

are much higher. Specifically, for the diameter of 9.9 Å, pressure drops of 74.2 MPa and 87.6 MPa are required for q = -9e and q = -12e, respectively at the specified water flow rate. For the diameter of 11.57 Å, required pressure drops are 44.1 MPa and 61.8 MPa for q = -9e and -12e, respectively. All these pressure drops are much higher than 35.02 MPa, which is associated with the case 9.9 Å pore diameter uncharged graphene membrane with 100% salt rejection efficiency [s1].

SI References

S1. C. T. Nguyen and A. Beskok, *The Journal of Chemical Physics*, 2018, **149**, 024704.
S2. J. Lyklema, *Colloids and Surfaces A: Physicochemical and Engineering Aspects*, 2006, **291**, 3-12.
S3. R. Qiao and N. Aluru, *Physical Review Letters,* 2004, **92**, 198301.
S4. M. Rezaei, A. Azimian and D. T. Semiromi, *Heat and Mass Transfer*, 2015, **51**, 661-670.
S5. Q. Cao and R. R. Netz, *Electrochimica Acta*, 2018, **259**, 1011-1020.